Nuclear Instruments and Methods in Physics Research B 512 (2022) 76–82

Contents lists available at ScienceDirect

Nuclear Inst. and Methods in Physics Research, B

journal homepage: www.elsevier.com/locate/nimb

First "Skin Depth" estimations using GEANT4 and FLUKA based simulations for CERN secondary beamlines

Gian Luigi D'Alessandro [a,b,*], Dipanwita Banerjee [a], Lau Gatignon [a], Johannes Bernhard [a], Alexander Gerbershagen [a], Maarten van Dijk [a,c], Stephen Gibson [b]

[a] CERN, Meyrin, Switzerland
[b] Royal Holloway, University of London, Egham, UK
[c] École Polytechnique Fédérale de Lausanne (EPFL), Lausanne, Switzerland

ARTICLE INFO

Keywords:
Accelerator Physics
Collimators
Particle physics
Secondary beamlines
CERN
North and East Area
Skin Depth

ABSTRACT

In order to have highly flexible secondary beamlines collimation is crucial. Collimators are blocks of material placed along the beamline that let the main beam pass within the collimator aperture limits, while most of the particles beyond it interact in the material and gets absorbed or loses enough energy to be deflected away from the beam core by the magnets placed downstream. Some particles can interact at the edge of the collimators and be accepted within the main beam, creating background for the experiments downstream. The thickness of the layer contributing to this potential background is called Skin Depth. It depends on the material of the collimator, on the beam momentum as well as the acceptance of the beamline in terms of momentum band and divergence. This article presents the first studies with GEANT4 and FLUKA based simulations on the effects of such interactions at the CERN secondary beamlines.

1. Introduction

The CERN secondary beamlines in the North [1] and the East Area [2] are designed to deliver beams of secondary and tertiary particles as well as attenuated primary protons and ions from the SPS and PS accelerators, see Fig. 1. The experimental areas of the SPS North Area comprises two surface halls, EHN1 and EHN2, as well as an underground cavern, ECN3. The beamlines deliver secondary and tertiary beams of hadrons, electrons and muons in the energy range < 360 GeV/c at a maximum flux of 10^7–10^8 particles/spill to these areas. Primary beams are attenuated to similar intensities in the surface halls as well. The East Area delivers beams of mixed as well as pure hadrons, electrons and muons in the momentum range < 15 GeV/c at a maximum flux of 5×10^6 particles/spill. In order to provide flexibility in momentum spread, beam flux, beam spot size and beam divergence, depending on the requirements of the downstream experiments, each beamline is equipped with a collimation system whose aperture settings can be modified.

Secondary beamline collimators are made of heavy materials with a high stopping power that are used to either define the acceptance or momentum of the beam or as a "cleaning collimators" to absorb the secondary particles that escape the acceptance collimator placed upstream. These collimators can have adjustable apertures in either one or two planes, respectively, and come also in a version with fixed aperture. The main beam passes within the aperture limits while the particles beyond its acceptance interact in the material. The collimator lengths range between 5–10 λ, where λ is the nuclear interaction length of the material. In hadronic cascades the length scale is a nuclear interaction length, λ, while in electromagnetic showers it is a radiation length, X_0 [4]. If the particles interact close to the edge of the collimator, lose a small amount of energy and still are accepted within the main beam, they contribute to tails in the transverse beam distribution and lead to potential backgrounds for the downstream experiments. The mean depth of the collimator material that is responsible for such effects will be referred to as the "Skin Depth" (please see the following section for a more detailed definition). As these effects play an important role in the design of the collimation system in a beamline, the skin depth for different materials was studied for charged and neutral particle beams at different incident momenta and for different beam acceptance. The impact of the alignment of the collimators on the "Skin Depth" calculation was not taken into account for these studies which aims to give a first estimation of this parameter for the secondary beamlines at CERN.

For these studies, straight jaw collimators have been considered, which are composed of one material only, i.e. no coating has been taken into account. The studies have been carried out with the help of FLUKA [5–7] and GEANT4 [8]. In this paper a brief overview of the

* Corresponding author at: CERN, Meyrin, Switzerland.
E-mail address: gianluigi.dalessandro@cern.ch (G.L. D'Alessandro).

https://doi.org/10.1016/j.nimb.2021.11.021
Received 13 September 2021; Received in revised form 11 November 2021; Accepted 28 November 2021
Available online 24 December 2021

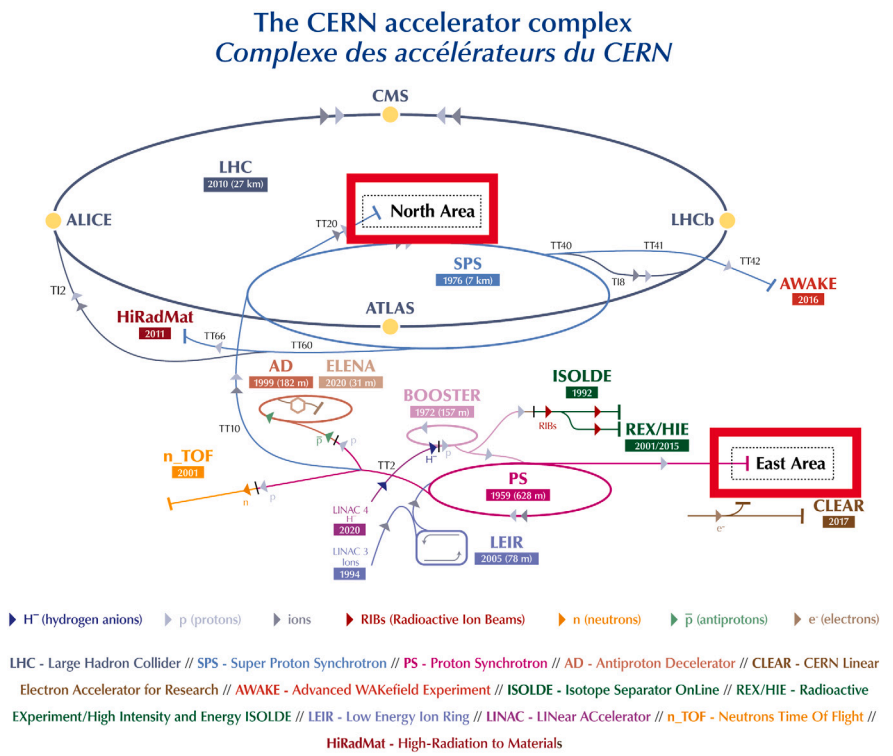

Fig. 1. CERN accelerator complex including the North and East Areas highlighted in red [3]. (For interpretation of the references to colour in this figure legend, the reader is referred to the web version of this article.)

collimation design principles for secondary beamlines is followed by the details of the simulation. The results and estimation for the skin depth are also presented in this paper.

2. Collimation at secondary beamlines

Primary protons impinging on a primary target produce secondary particles, while a fraction escapes from the target without inelastic or quasi-elastic interactions. The majority of the particles emerging from the target are not useful for experiments and must be stopped as soon as possible, while the rest are transported through the downstream beamline. In the North Area, for example, the primary protons have a momentum of 400 GeV/c and several 10^{12} or up to more than 10^{13} of them impinge on each of the primary targets per extraction. In most cases only a few 10^{8} or less are finally selected. Therefore, a large share of the energy contained in the beam is deposited on the primary TAX dump-collimator (Target Attenuator eXperimental areas). This collimator is placed right after the target following a dipole magnet or at a production angle to allow the passage of the selected beam. This beam is then transported along the secondary beamlines through a series of collimators to the experiments downstream.

Materials used in the secondary beamline collimators vary according to applications. For example, tungsten has a nuclear interaction length of approximately 10 cm and therefore has a high stopping power. This combined with some thermodynamical properties, like a high melting point, makes it a suitable material for the collimator jaws along the apertures. The bulk materials are usually steel or copper. Materials commonly used are listed in Table 1. Some general design considerations for the collimation systems of charged and neutral particle beamlines are presented in the following sections, along with some examples from the CERN North Area [9].

2.1. Charged particle beam collimation

When a collimator is placed in a charged particle beam, the beam core is accepted within the aperture limits, however the rest of the particles will interact in the collimator material and produce secondary particles which are either absorbed in the material or escape the collimator following further interactions. Most of these secondary particles escaping from the collimator have low energy and can cause significant background for the experiments if not mitigated properly. Some of these interactions also produce neutral hadrons and photons which are harder to suppress. In order to deal with lower energy charged particles, the collimators are normally followed by a number of additional cleaning collimators as well as magnets, i.e. dipoles or quadrupoles. These magnets, if tuned according to the nominal beam momentum, will sweep the lower energy charged debris away from the downstream experiment. However, muons are minimally affected by the normal collimators. Indeed the typical dE/dx for muons in iron is about 1.5 GeV/m. Therefore, for muons magnetised collimators with toroidal field are used. These collimators, called Scrapers, help to deflect away the muons passing through the yoke without affecting the beam core. In order to give an additional kick and sweep these muons away from the beam core, the Scrapers are complemented with more massive toroids called Magnetised Iron Blocks (MIBs). All these magnetic sweeping requires a long lever arm. Therefore, as a general rule it is important to implement strong collimation as early as possible in the beamline.

Table 1
Materials commonly used for collimation at the CERN secondary beamlines with their respective values of nuclear interaction length, radiation length, density and stopping power [10]. The iron and tungsten used, however, are alloys with a small percentage of light materials and the values correspond to that.

Material	λ_I (cm)	X_0 (cm)	ρ (g/cm^3)	$\frac{dE}{dx}$ (MeV/cm)
Be	42.1	35.2	1.8	2.9
Al	39.7	8.9	2.7	5.4
Fe	18.3	1.9	7.2	11.4
Cu	15.3	1.4	8.9	12.6
Pb	17.6	0.6	11.4	12.7
W	10.7	0.4	18.0	22.1

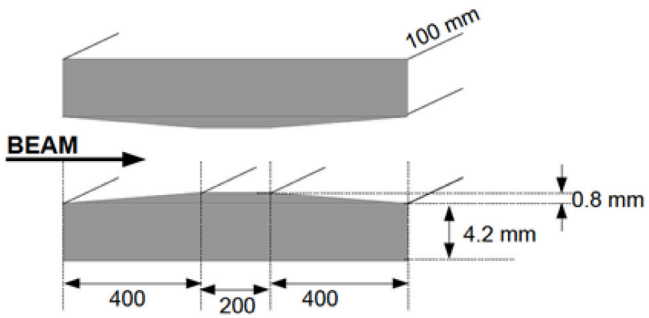

Fig. 2. Profile of the jaws of Collimator 3 of the K12 beamline with copper shim plates.

The standard collimators in secondary beamlines at CERN are typically about 1 m long, much shorter than typical focal distances in charged particle beamlines at high energies. Therefore, collimator jaws are normally flat blocks. However, if a collimator is known to always have a very small aperture and if it is located in a very sharp focus, it may be of interest to shape the collimator jaws accordingly. An example of such a case for a charged beam is Collimator 3 in the K12 beamline for the NA62 experiment [11], which has a nominal aperture of ±1.2 mm with tapered jaws before and after a flat section, as shown in Fig. 2, including copper shim plates.

2.2. Neutral particle beam collimation

As for charged particle beams, in neutral particle beamlines all collimators must be followed by sweeping dipoles, as interactions of neutral particles (hadrons or photons) will produce charged interaction products. In general, charged particle transport has to be suppressed further down a neutral particle beamline, so the magnets should be as strong as reasonably achievable, while ensuring that they have a comfortably larger aperture than the neutral beam core. The more upstream the charged particles can be swept away the better, in particular pions and kaons, which can decay into muons pointing to the experiment and which are hard to suppress. However, neutral particle beam collimation is more delicate than charged particle beam collimation. Neutral hadrons impinging on a collimator will be more likely to undergo strong nuclear interactions inside the material and their interaction products, charged or neutral, may leave the collimator jaw with wide angular and momentum spreads. Charged particles can be swept away magnetically, but neutrals cannot. Mitigation is then only achievable by means of multiple collimation stages, each in turn affected by the skin depth of the collimators used, ideally with sweeping magnets at each collimation stage.

2.3. Skin depth

In addition to the part of the beam that interacts with the bulk of the collimator material and loses significant energy and can be swept away with the dipole magnets, there may also be particles that interact very close to the collimator edge and lose a small amount of energy. These can remain within the beam core depending on the momentum acceptance of the beamline. This is characterised by the impact parameter called "Skin Depth". It is the mean thickness of the layer at the collimator edge at which the beam impacts, loses a small amount of energy and then scatters back into the collimator aperture to be accepted within the main beam and cause potential background. The distribution of the initial impact position of such particles that finally emerge from the collimator edge and are accepted within the beam core follows an exponential function, $\alpha e^{-\alpha x}$, where α is the decay parameter. The skin depth (δs) is calculated from this distribution with a cut at 90% of the population as:

$$\delta s = \frac{ln(10)}{\alpha} \approx \frac{2.3}{\alpha} \quad (1)$$

The factor $ln(10)$ comes from a cut accepting 90% of the distribution. For a given skin depth of value δs and a collimator with aperture of size a, the effective aperture of the collimator, considering skin depth corrections, will be $a + \delta s$. It is important to take this into account to mitigate scattering products from the collimators creating backgrounds and tails for the experiment.

In order to characterise the skin depth for different materials, incident momenta, and acceptance, GEANT4 and FLUKA based simulations have been performed. Details and results are presented in the following section.

3. Skin depth estimations for charged and neutral particle beam

The geometry description of the FLUKA and GEANT4 models created for these skin depth studies is based on a simple block that represents a single collimator jaw. The block spans 80 cm in X and Y and has a length of 1 m in Z. It spans the plane 0 cm≤X≤80 cm, -40 cm≤Y≤40 cm and -50 cm≤Z≤50 cm. The incident beam has a flat spatial distribution of 0–8 mm in X with zero spread in Y which is sufficient to estimate the skin depth values in the order of a few hundred microns corresponding to one plane (X). The angular spread is set to $\sigma_{X'_0} = 5$ mrad and $\sigma_{Y'_0} = 0$ mrad to include the maximum angular acceptance of most CERN Secondary beamlines. The model is shown in Fig. 3 in the GEANT4 visualiser for an example of five incident π^+ particles following the above distribution and interacting in the collimator jaw. The particle tracks are identified by colour as shown in the table enclosed in the figure. The skin depth is calculated for different incident momenta, p_0, where the chosen values are representative of the CERN North Area. The number of events simulated in both GEANT4 and FLUKA is 10^6.

The version of GEANT4 used for the simulation is GEANT4.10.06 using the complete $FTFP\_BERT$ physics lists. It uses the Fritiof string model and the Bertini cascade model. The Fritiof (FTF) model assumes that one or two unstable objects — quark-gluon QCD-strings, are produced in elementary interactions. It propagates the interactions assuming that these objects can interact with other nucleons in hadron–nucleus and nucleus–nucleus collisions, and can increase their masses [12]. The Bertini (BERT) model is used for parametrisation of the intranuclear cascade of hadrons and nucleons produced through a series of interactions within the nucleus [13].

The FLUKA version used is 4-0.1 with FLAIR 3.1-2 with a DEFAULTS card set to PRECISIO (an option that includes more detailed electromagnetic and hadronic processes leading to a higher precision), without further cuts and using the standard FLUKA physics list. The standard FLUKA physics list distinguishes among three main hadronic interaction types: hadron-nuclear inelastic interaction, elastic scattering and nucleus–nucleus interaction. Quasi-elastic processes are a minor share of processes and are not discussed here, for more detail on these see [14]. The hadron-nuclear uses at momenta below 3–5 GeV/c a package that includes a very detailed Generalised Intra-Nuclear Cascade and a pre-equilibrium stage [15], while at high energies it exploits the

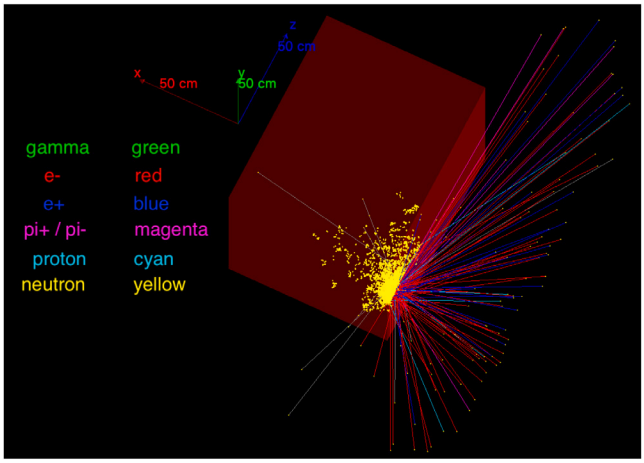

Fig. 3. Visualisation from the GEANT4 model for the collimation studies showing five incident π^+ particles interacting in the collimator jaw. The particles in the shower are identified by colour as described in the table inserted in the figure.

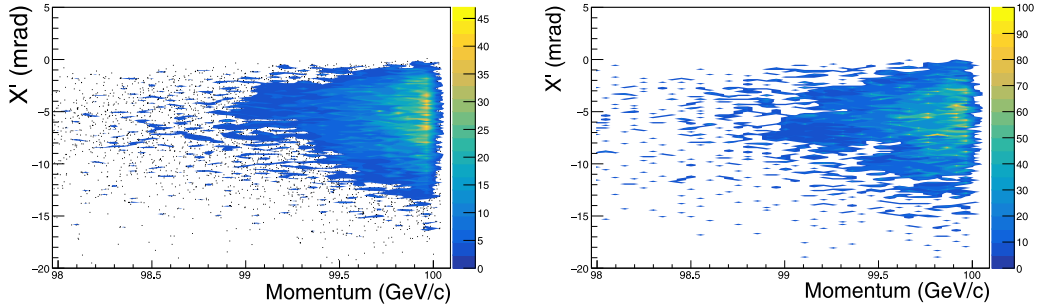

Fig. 4. Distribution of the angle (mrad) vs momentum (GeV/c) for the charged particles that interact at the edge of the 1 m long tungsten collimator and that are accepted within the aperture limits for a 100 GeV/c incident π^+ beam from GEANT4 (left) and FLUKA (right).

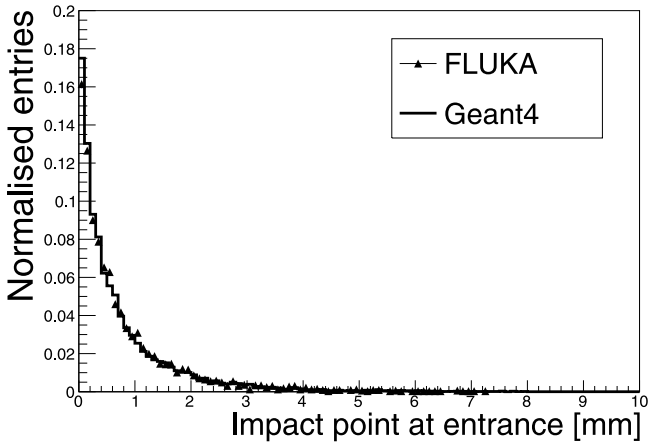

Fig. 5. The distribution of the impact point of the 100 GeV/c π^+ particle for events where a charged particle scatters off the collimator material and is accepted within the aperture limits for a 1 m long tungsten collimator from GEANT4 and FLUKA.

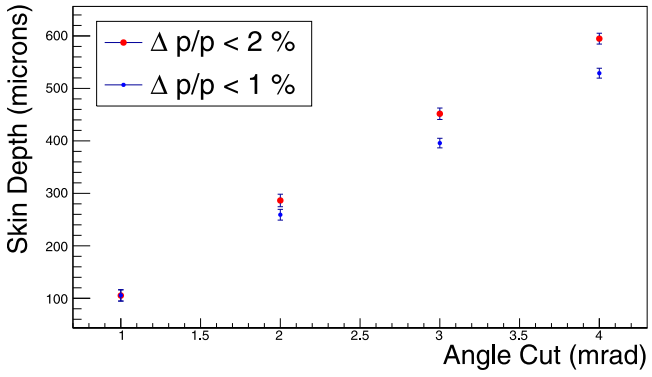

Fig. 6. Skin Depth as a function of the angle cut for $\Delta p/p < 2\%$ and $\Delta p/p < 1\%$ from GEANT4 for a tungsten collimator.

Gribov–Glauber multiple collision mechanism [16]. For elastic scattering FLUKA uses a series of parameterised and tabulated interactions. Finally for nucleon–nucleon interaction above 5 GeV per nucleon it uses DPMJET-II or DPMJET-III [17], between 0.1 and 5 GeV the modified Relativistic Quantum Molecular Dynamics [18] and below 0.1 GeV the Boltzmann Master Equation [19]. The results from the different runs in the two simulation packages are summarised below.

3.1. Charged particle beam

To estimate the skin depth relevant for charged particle beamlines a π^+ beam was simulated following the aforementioned distributions. All charged particles that leave the collimator block before the end of the 1 m and reach the X<0 m region are scored. The distribution of these outgoing particles for a 100 GeV/c π^+ beam incident on a 1 m tungsten block in the X' vs momentum space is presented in Fig. 4 from GEANT4 and FLUKA respectively.

The outgoing beam has a low energy tail which can potentially create background for the downstream experiments. The distribution of the initial impact points of the primary π^+ beam on the collimator for the events with such outgoing particles is shown in Fig. 5.

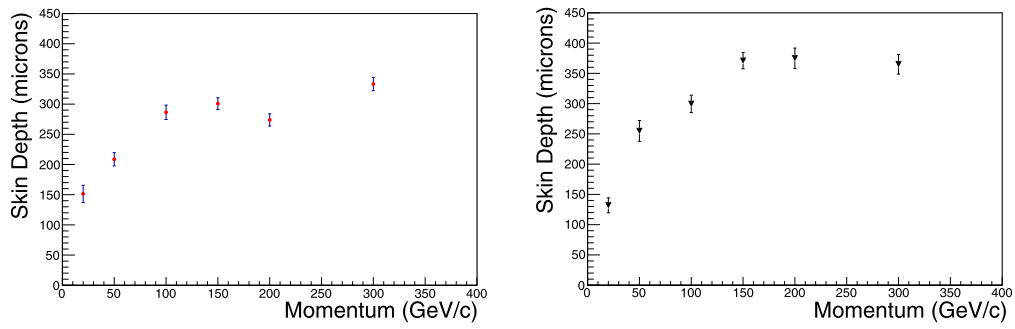

Fig. 7. Skin Depth calculated for different momenta using a cut of $\Delta p/p < 2\%$ and an angular cut of 2 mrad in X' and Y' from GEANT4 (left) and FLUKA (right) for a tungsten collimator.

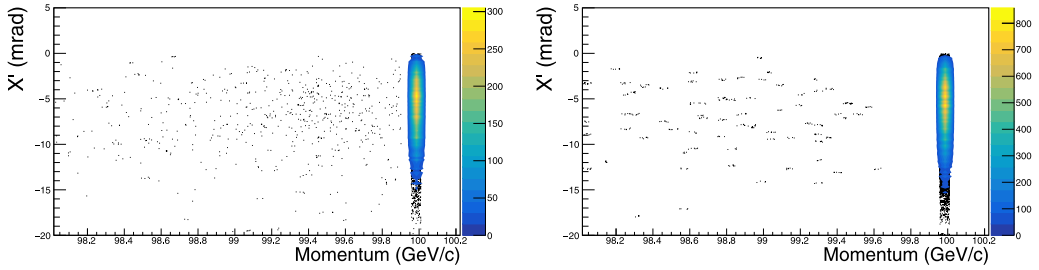

Fig. 8. Distribution showing the angle (mrad) vs momentum (GeV/c) for the neutral particles that interact at the edge of the collimator for a 1 m long Tungsten block and are accepted within the aperture limits for a 100 GeV/c incident K_L beam from GEANT4 (left) and FLUKA (right).

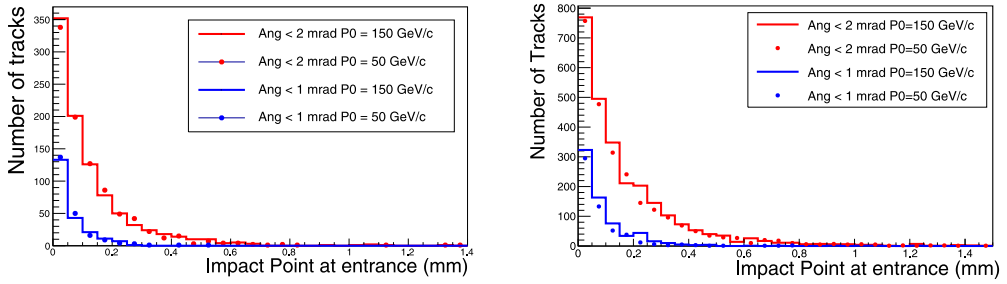

Fig. 9. Distribution of impact point for 50 GeV/c and 150 GeV/c incident momenta K_L beam, for events where scattered neutral particles are accepted within the aperture limits for two angular cuts of 1 mrad and 2 mrad from GEANT4 (left) and FLUKA (right).

The distributions from the two software packages are in very good agreement. However, not all of these particles interacting with the collimator material and accepted within the aperture will be transported through the rest of the beamline. The downstream bending magnets will sweep away the lower energy tails. The resulting skin depth, therefore, depends on the acceptance used for the cuts. This was estimated from the slope α of the exponential distribution as shown in Fig. 5, after applying the acceptance cuts, according to Eq. (1). Fig. 6 shows the calculated skin-depth for a 100 GeV/c incident pion beam on a 1 m tungsten block as a function of different angular and momentum acceptance cuts. As seen, the skin depth is more sensitive to the angular than the momentum cut, as expected at these energies. Following this a reasonable cut on the momentum of $\Delta p/p < 2\%$ and divergence within 2 mrad was set on the outgoing particles to also estimate the Skin Depth of the materials for the different incident momenta. Fig. 7 shows the Skin Depth as a function of the incident momenta for a tungsten collimator. As seen the skin depth is directly correlated with the incident momenta for the lower momentum values but the effect reduces and the skin depth plateaus for momenta greater than about 100 GeV/c.

The Skin Depth values were also calculated for different materials using a 100 GeV/c π^+ beam and the aforementioned cuts. These results are summarised in Table 2.

Table 2
Skin Depth for a 100 GeV/c incident π^+ beam for different materials calculated in FLUKA and GEANT4.

Material	*GEANT*4 (μm)	*FLUKA* (μm)
Be	1106 ± 16	1092 ± 16
Al	1005 ± 15	964 ± 17
Fe	598 ± 16	616 ± 16
Cu	575 ± 14	508 ± 14
Pb	577 ± 15	556 ± 16
W	322 ± 11	306 ± 10

In this case the skin depth is strongly correlated with the nuclear interaction length of the material as expected, with the values being larger for larger nuclear interaction lengths.

3.2. Neutral particle beam

For the neutral particle beam estimations, a 100 GeV/c K_L beam was simulated with the same distribution and geometry as for the charged particle beam. The charged interaction products were ignored for the studies, as they would be removed by magnetic sweeping [20]. Fig. 8 shows the distribution of angle versus momentum of the neutral

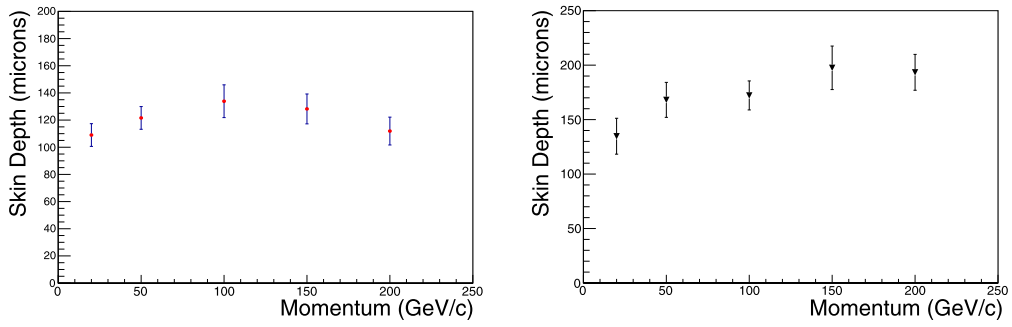

Fig. 10. Skin Depth for K_L beam incident on a 1 m long tungsten block at various momenta for an angular cut of 1 mrad from GEANT4 (left) and FLUKA (right).

Table 3
Skin Depth for 100 GeV/c K_L beam for different materials calculated in GEANT4 and FLUKA.

Material	*GEANT*4 (μm)	*FLUKA* (μm)
Be	565 ± 19	565 ± 18
Al	575 ± 20	550 ± 21
Fe	331 ± 22	351 ± 21
Cu	248 ± 19	287 ± 17
Pb	225 ± 18	310 ± 16
W	138 ± 12	180 ± 10

particles leaving a 1 m tungsten collimator in the X <0 region, for GEANT4 and FLUKA, respectively.

Since the neutral particles are not affected by the bending magnets, a momentum cut is not reasonable in this case. Only an angular cut was therefore used to estimate the Skin Depth for different materials for a neutral beam. Fig. 9 shows the distribution of the impact point for the events where the incident beam is accepted within the aperture limits of the collimators after interaction, for two different incident momenta (50 and 150 GeV/c) and angular cuts (1 mrad and 2 mrad). As seen from both software the dependence of the distribution is stronger on the angular cut than the incident momentum. The distribution differs considerably between the two angular cuts for the same incident momentum, e.g., 1 mrad and 2 mrad for a 150 GeV/c incident momentum, but is almost identical for the different incident momenta and same angular cut.

In a next step the Skin Depth value was checked as a function of the incident momenta for an angular cut of 1 mrad as shown in Fig. 10, which also does not show strong dependence on the incident momenta for the range of values studied.

In addition we calculated the Skin Depth for the different materials. Table 3 shows the values for some commonly used materials for a 100 GeV/c incident K_L beam and an angular cut of 1 mrad for the accepted particles.

3.3. Applications of skin depth studies

Some studies on skin depth were developed for the collimation system of the NA48 experiment in the past. These studies helped in the design and development of this beamline that made use of a K_Ls beam and a collimation system based on momentum defining, acceptance and cleaning collimators [21]. The positions of these were calculated precisely using the skin depth as explained before. An experiment using a K_L beam is currently being investigated within the Physics Beyond Colliders (PBC) studies at CERN [22] called KLEVER [20]. It aims to use a K_L beam as well and for this experiment the characterisation of the Skin Depth to design the collimation system is once again fundamental for a successful run. In particular, to select the material that would best suit the collimation needs of the experiment knowing the value of the skin depth parameter is crucial.

4. Conclusion

This paper summarises the effect of the interaction of secondary beams in the collimation system and the impact parameter "Skin Depth" for different incident momenta and materials. First detailed simulation studies have been performed for charged and neutral particle beams at the CERN North Area to estimate this parameter in order to mitigate the background from the scattered products for the downstream experiments. It has been shown that skin depth is directly correlated with the nuclear interaction length of the material for both neutral and charged particles. Skin depth does not depend strongly on the initial beam momentum for P_0 > 100 GeV/c but varies considerably with the beamline acceptance, e.g., the momentum and angular cuts. These considerations are fundamental for precise beamline design for the secondary beams as is currently being done for KLEVER. These studies are also useful for material activation studies, topic of particular interest for high-energy proton accelerators. Although some studies on this impact parameter and beam collimation have already been done in the past, e.g., for NA48 as well as in the context of colliders [23,24], no exhaustive studies have been developed before for secondary beamlines with a precise definition of skin depth. Simulations presented in this article show a good agreement between GEANT4 and FLUKA providing a useful input for future design of collimators in the CERN East and North Area and can be extended to other beams that use a similar energy range. Further investigations on the effects of collimator misalignment on the skin depth values are being carried out and will be presented in future.

CRediT authorship contribution statement

Gian Luigi D'Alessandro: Writing – original draft, Data curation, Software, FLUKA-simulations. **Dipanwita Banerjee:** Writing – original draft, Data curation, Software, Geant4-simulations. **Lau Gatignon:** Conceptualization, Methodology. **Johannes Bernhard:** Supervision, Reviewing and editing. **Alexander Gerbershagen:** Supervision, Reviewing and editing. **Maarten van Dijk:** Conceptualization, Software, Reviewing and editing. **Stephen Gibson:** Supervision.

Declaration of competing interest

The authors declare that they have no known competing financial interests or personal relationships that could have appeared to influence the work reported in this paper.

References

[1] D. Banerjee, et al., The North Experimental Area at the CERN supper proton synchrotron, in: CDS-CERN DOCUMENT SERVER, CERN-ACC-NOTE-2021-0015, 2021, URL http://cds.cern.ch/record/2774716.
[2] S. Evrard, et al., East Area Technical Design Report, To Be Published As CERN Yellow Report, 2021.
[3] E. Mobs, The CERN accelerator complex - 2019., 2019, URL https://cds.cern.ch/record/2684277.

[4] N.V. Mokhov, F. Cerutti, Beam-material interaction, in: Proceedings of 2014 Joint International Accelerator School: Beam Loss and Accelerator Protection, Newport Beach, CA, USA, 2014, http://dx.doi.org/10.5170/CERN-2016-002.83.
[5] G. Battistoni, et al., Overview of the FLUKA code, Ann. Nucl. Energy 82 (2015) 10–18, http://dx.doi.org/10.1016/j.anucene.2014.11.007.
[6] T.T. Boehlen, et al., The FLUKA code: Developments and challenges for high energy and medical applications, Nucl. Data Sheets 120 (2014) 211–214, http://dx.doi.org/10.1016/j.nds.2014.07.049.
[7] V. Vlachoudis, FLAIR: a powerful but user friendly graphical interface for FLUKA, in: Proceedings of International Conference on Mathematics, Computational Methods and Reactor Physics (M&C 2009), NY, USA, 2009, pp. 1–4, https://cds.cern.ch/record/2749540.
[8] S. Agostinelli, et al., Geant4—a simulation toolkit, Nucl. Instrum. Methods Phys. Res. A 506 (3) (2003) 250–303, http://dx.doi.org/10.1016/S0168-9002(03)01368-8.
[9] L. Gatignon, Design and tuning of secondary beamlines in the CERN north and east areas, CERN-ACC-NOTE-2020-0043, CERN Document Serv. (2020) 33–48, URL http://cds.cern.ch/record/2730780.
[10] P.A. Zyla, et al., Particle data group, Prog. Theor. Exp. Phys. 2020 (8) (2020) 144–146, http://dx.doi.org/10.1093/ptep/ptaa104.
[11] F. Hahn, NA62 collaboration, NA62: TEchnical design document, CDS-Cern Doc. Serv. (2010) 414, URL https://cds.cern.ch/record/1404985.
[12] V. Uzhinsky, behalf of the Geant4 Hadronics Working Group, Development of the Fritiof Model in Geant4, in: Joint International Conference on Supercomputing in Nuclear Applications and Monte Carlo 2010, Tokyo, Japan, 2010, pp. 1–4, https://inis.iaea.org/search/search.aspx?orig_q=RN:43053486.
[13] D.H. Wright, M.H. Kelsey, GEANT4 Hadronics Working Group, The Geant4 bertini cascade, Nucl. Instrum. Methods Phys. Res. A (2015) 175–188, http://dx.doi.org/10.1016/j.nima.2015.09.058.
[14] A. Lechner, Particle interactions with matter, in: CAS - CERN Accelerator School: Beam Injection, Extraction and Transfer, Erice, Italy, 2017, pp. 47–66, http://dx.doi.org/10.23730/CYRSP-2018-005.47.
[15] A. Fasso', et al., New developments in FLUKA modelling hadronic and EM interactions, in: Proceedings of the Third Workshop on Simulating Accelerator Radiation Environments, Hyrayama, Japan, 1997, pp. 1–6, https://inis.iaea.org/search/search.aspx?orig_q=RN:30045529.
[16] A. Ferrari, P. Sala, Nuclear reactions in Monte Carlo code, Radiat. Prot. Dosim. 99 (1-4) (2002) 29–38, http://dx.doi.org/10.1093/oxfordjournals.rpd.a006788.
[17] S. Roesler, et al., The Monte Carlo event generator DPMJET-III, in: International Conference on Advanced Monte Carlo for Radiation Physics, Lisbon, Potugal, 2000, pp. 1–6, http://dx.doi.org/10.1007/978-3-642-18211-2_166.
[18] H. Sorge, et al., Poincaré invariant Hamiltonian dynamics: Modelling multi-hadronic interactions in a phase space approach, Ann. Phys. 192 (2) (1989) 266–306, http://dx.doi.org/10.1016/0003-4916(89)90136-X.
[19] A. Fasso', et al., The physics models of FLUKA: status and recent developments, in: Proceedings of CHEP03, la Jolla, California, 2003, pp. 1–9, https://cds.cern.ch/record/625976.
[20] M.W.U. van Dijk, et al., The K12 beamline for the KLEVER experiment, in: Proceedings of IPAC2019, Melbourne, Australia, 2019, pp. 3726–3729, http://dx.doi.org/10.18429/JACoW-IPAC2019-THPGW061.
[21] C. Biino, et al., The simultaneous long and short-lived neural kaon beams for experiment NA48, CERN-NA48-NOTE-98-16, CDS-Cern Doc. Serv. (1998) 8–9, URL http://cds.cern.ch/record/359229.
[22] L. Gatignon, et al., Report from the conventional beams working group to the physics beyond colliider study and to the European strategy for particle physics, CERN-PBC-REPORT-2018-002, CDS-CERN Doc. Serv. (2018) 75–88, URL https://cds.cern.ch/record/2650989.
[23] A.W. Chao, M. Tigner, Handbook of Accelerator Physics and Engineering, World Scientific Publishing, 2009, pp. 244–249, http://dx.doi.org/10.1142/8543.
[24] V. Boccone, et al., Beam-machine interaction at the CERN LHC, Nucl. Data Sheets 120 (2014) 215–218, http://dx.doi.org/10.1016/j.nds.2014.07.050.